Thermodynamic and Spectroscopic Characterization and *in vitro* O_2^- Scavenger Activity of Copper(II) Glycyl-L-histidyl-glycyl-L-histidine Complexes *

Raffaele P. Bonomo,[a] Francesca Bonsignore,[b] Enrico Conte,[a] Giuseppe Impellizzeri,[a] Giuseppe Pappalardo,[b] Roberto Purrello[a] and Enrico Rizzarelli[a,b]

[a] *Dipartimento di Scienze Chimiche, Università di Catania, V. le A. Doria 6, 95125 Catania, Italy*

[b] *Istituto per lo Studio delle Sostanze Naturali di Interesse Alimentare e Chimico Farmaceutico, CNR, V. le A. Doria 6, 95125 Catania, Italy*

Thermodynamic and spectroscopic (electron spin resonance, electronic and circular dichroism) studies have been carried out on the complex species which exist in the copper(II)–glycyl-L-histidyl-glycyl-L-histidine (HL) system in aqueous solution. The thermodynamic results suggest the formation of three important species: $[CuL]^+$, $[CuH_{-1}L]$ and $[CuH_{-2}L]^-$, the first being present in the range pH 3.0–5.5, the second and third in different ratios between pH 5.5 and 7.8. The complex $[CuL]^+$ has a pseudo-octahedral structure, the equatorial plane of which involves the amino group, the first peptide nitrogen, an imidazole nitrogen and a water molecule; $[CuH_{-1}L]$ has the same donor atoms in the equatorial plane and the other imidazole nitrogen binds in an apical site, giving a square-pyramidal geometry. For $[CuH_{-2}L]^-$, in which a second peptide nitrogen is deprotonated, the geometry is distorted and can be considered intermediate between a square pyramid with a tetrahedrally distorted plane and a distorted trigonal bipyramid. *In vitro* O_2^- scavenging experiments show that the most active species is $[CuH_{-2}L]^-$. The superoxide dismutase-like activity has been rationalized by considering the geometry of the copper(II) complex species.

It is well known that the histidyl residue is a relevant bonding site for the copper(II) ion in a number of metalloenzymes.[1–4] Furthermore, this residue is present in low molecular weight complexes that serve as delivery systems of copper(II) to tissues or that alter the growth rate or the state of differentiation of cultured cells and organisms.[5–7] This biological relevance explains the number of studies on the co-ordination properties of histidine-containing peptides. However, mainly metal complexes of oligopeptides containing one histidyl residue have been investigated.[8–13] Some results on the interaction of copper(II) with linear[14,15] and cyclic peptides[16,17] with two histidyl residues have only recently been reported, in an attempt better to mimic the binding mode of the histidyl residue in metalloenzymes.

The reactivity of histidine-containing copper(II) di- or tripeptide complexes toward O_2^- radicals has also been investigated.[18–20] The different superoxide dismutase-like activity has been correlated with the copper(II) complex geometries, as a result of the different positions of the histidyl residue along the peptide chain, as well as with the type of donor atoms and the strength of the ligand fields.

Herein we report the synthesis of the tetrapeptide glycyl-L-histidyl-glycyl-L-histidine and its complexation with copper(II). The species formed in the pH range investigated are determined by potentiometric measurements and the co-ordination features of the species present in solution inferred using electron spin resonance (ESR), visible absorption and circular dichroism (CD) spectroscopies. Also superoxide dismutase-like activities (obtained by an indirect assay[21]) of the species present at physiological pH values are correlated with the peculiar arrangement of donor atoms around the copper(II) ion.

Experimental

Synthesis and Materials.—The tetrapeptide HL was synthesised on a Milligen/Biosearch 9050 peptide synthesizer using *N*-(9-fluorenylmethoxycarbonyl) (fmoc) amino acid pentafluorophenyl esters (Millipore). The peptide was assembled starting from fmoc-His-(boc)-Pepsyn KA (Millipore) resin (boc = *tert*-butoxycarbonyl) and cleaved from the resin with 95% trifluoroacetic acid (tfa) in water. The product was purified on a CM Sephadex C-25 (NH_4^+ form) column, which was eluted with a linear gradient from 0 to 0.1 mol dm^{-3} aqueous ammonium hydrogen-carbonate. The tetrapeptide purity was checked (*i*) by high-performance liquid chromatography over Spherisorb ODS-2 (5 μm) in a 125 × 4 mm column with a linear gradient of water–MeCN (0:30%) containing 0.1% tfa (detection at 220 nm) and (*ii*) by potentiometric titrations with standard KOH solution. The purity always proved to be higher than 99.5% and the amino acid analysis data were consistent with the expected sequence and ratios; m.p. 184–186 °C, α(589.3 nm, 25 °C, *c* 1.0 g 100 cm^{-3} in H_2O) = +7.5°. FAB mass spectrum: *m/z* 407 $(M + H)^+$ (Found: C, 47.30; H, 5.40; N, 27.40. Calc. for $C_{16}H_{22}N_8O_5$: C, 47.30; H, 5.50; N, 27.50%).

Copper(II) nitrate was a 'reinst' Merck product. The concentrations of stock solutions were determined by ethylenediaminetetraacetate titrations using murexide as indicator.[22] Stock solutions of HNO_3 and KOH were made up from concentrated HNO_3 (Suprapur Merck) and from Normex C. Erba vials respectively, and their concentrations were determined potentiometrically by titrating with tris(hydroxymethyl)methylamine and potassium hydrogenphthalate respectively. All solutions were prepared with freshly distilled (four times) CO_2-free water. The ionic strength was adjusted to 0.10 mol dm^{-3} by adding KNO_3 (Suprapur Merck). Grade A glassware was employed throughout. Xanthine, xanthine oxidase and nitro blue tetrazolium (nbt) were from Sigma.

Electromotive Force Measurements.—The potentiometric measurements were carried out using two fully automated sets of apparatus, incorporating Metrohm equipment (burette, E665; meter, E654; combined electrode, EA125) which were controlled by an IBM compatible PC and a program written in

* *Non-SI unit employed:* G = 10^{-4} T.

Table 1 Experimental conditions for potentiometric measurements at 25 °C (I = 0.1 mol dm^{-3})

$c°_M$/ mmol dm^{-3}	$c°_L$/ mmol dm^{-3}	Titrant KOH/ mol dm^{-3}	pH Range	Number of points
—	3.91	0.099 98	2.1–8.5	46
—	3.91	0.1001	2.1–8.4	46
—	4.89	0.099 98	2.3–8.7	48
—	4.89	0.1001	2.3–8.9	50
5.03	5.15	0.1006	3.0–6.5	42
5.03	5.15	0.1009	3.1–5.0	30
3.41	3.06	0.1006	3.1–6.0	39
3.41	3.06	0.1009	3.1–6.7	53
6.94	7.03	0.1006	3.0–6.7	40
6.94	7.03	0.1009	3.0–6.7	60

Table 2 Spectroscopic data for copper(II)–peptide complexes

	λ/nm	
	d–d[a]	
Complex	Absorbance maximum	CD[b]
$[CuL]^{+}$[c]	606 (58)	608 (0.34) 502 (−0.03) 330 (0.17)
$[CuH_{-1}L']$[d]	606 (55)	604 (0.04) 498 (−0.05) 335 (0.21)
$[CuH_{-1}L]$	574 (54)	
$[CuH_{-2}L]^{-}$	575 (72)	

[a] ε/dm^3 mol^{-1} cm^{-1} in parentheses. [b] Δε/dm^3 mol^{-1} cm^{-1} in parentheses. [c] This work. [d] Refs. 13 and 15, HL′ = Gly-L-His-Gly.

Table 3 Isotropic[a] and anisotropic[b] spin Hamiltonian parameters[c] associated with the complex species formed by the Cu–HL system on varying the pH of the solution.

pH	g_{iso}	A_{iso}[d]	A^{N}_{iso}[d]		
4.5–5.0	2.118(2)	76(2)	13(2)		
6.4	2.113(2)	73(2)	13(2)		
7.8	2.105(4)	70(2)	—		
Complex	$g_{\|\|}$	$A_{\|\|}$[d]	$g_{\perp}$	$A_{\perp}$[d]	
$[CuL]^{+}$	2.237(3)	193(2)	2.047(3)	20(4)	
$[CuH_{-1}L]$	2.268(2)	130(2)	2.070(2)	14(2)	
$[CuH_{-2}L]^{-}$	2.322(2)	143(2)	2.019(3)	11(3)	

[a] 298 K, water. [b] 150 K, water–methanol (85:15). [c] Presumed errors on the last digit in parentheses. [d] Hyperfine coupling constants in 10^4 cm^{-1}.

our laboratory. All experiments were carried out at 25.0 ± 0.2 °C using 5 cm^3 thermostatted cells. All solutions were stirred magnetically and maintained in an atmosphere of inert nitrogen previously saturated by bubbling through 0.1 mol dm^{-3} KNO_3 solutions. The electrode couples were standardized on the pH = $-\log c_H$ scale by titrating HNO_3 with CO_2-free KOH. Solutions containing the ligand and the ligand in the presence of copper(II) were titrated with standard KOH. Each experiment was run simultaneously on both sets of potentiometric apparatus to avoid systematic errors and to check for reproducibility. Experimental details for the potentiometric titrations are reported in Table 1. Other details are as previously reported.[17]

Calculations.—The calculations for calibrating the electrode system, together with values of the slope were performed using the ACBA program,[23] which refines the parameters of an acid–base titration by using a non-linear least-squares method minimizing the function $U = \Sigma(V_{exptl} - V_{calc})^2$, where V is the volume of titrant added. SUPERQUAD,[24] which minimizes the error-square sum based on measured electrode potentials, was used for all other data. The distribution diagram was obtained using DISDI.[25]

Spectroscopic Measurements.—Absorption spectra were recorded on a Hewlett-Packard HP 8452 spectrophotometer and CD spectra on a JASCO J-600 automatic recording spectropolarimeter. Both were recorded at room temperature under the same experimental conditions used for the potentiometric measurements. The results are summarized in Table 2.

First-derivative X-band ESR spectra were recorded on a conventional spectrometer (Bruker model ER 200 D), using a 100 kHz field modulation and a 10 in electromagnet. Quartz tubes were used to obtain spectra for frozen solutions at 150 K and a Bruker flat cell for aqueous solutions at room temperature. Powdered diphenylpicrylhydrazyl samples were used to calibrate the microwave frequency, while the magnetic field was measured using a Bruker gaussmeter (type ER 035M), which leaves markers at preselected values. The complex solutions were prepared from isotopically pure ^{63}Cu, and up to 15% methanol was added to the complex aqueous solution used for the room temperature experiments, in order to increase resolution of the frozen solution spectra. The spectra were recorded on varying the pH of the aqueous solutions from 4.5 to 7.8. For species present at pH *ca.* 7, spin Hamiltonian parameters were obtained by carefully simulating the experimental spectra using a program devised substantially by Pilbrow and Winfield.[26] The spin Hamiltonian parameters are reported in Table 3.

Hydrogen-1 NMR spectra were recorded on a Bruker 250 MHz spectrometer at 298 K in D_2O. The ^1H NMR spectrum of HL at room temperature in D_2O shows two broad signals in the aromatic region which can be attributed to the histidine side chains. At low temperature (278 K) there is almost complete resolution in the same region, probably due to the decreased rotational degree of the histidine side chains. A complete NMR study to elucidate the possible conformational states of the ligand is in progress and will be published elsewhere.

Superoxide Dismutase Activity Measurements.—Superoxide dismutase-like activity was determined indirectly using the method of Beauchamp and Fridovich.[21] Superoxide ions were generated by a xanthine–xanthine oxidase system and detected spectrophotometrically by monitoring the formation of formazan as the product of nbt reduction by O_2^- at 560 nm.

Reactions were carried out in nbt (100 μmol dm^{-3}) and xanthine (50 μmol dm^{-3}) in a phosphate buffer (10 mmol dm^{-3}) at pH 6.8 and 7.8. An appropriate amount of xanthine oxidase was added to 2 cm^3 of the reaction mixture to cause a change in absorbance (ΔA_{560}) of 0.024 min^{-1}, corresponding to a rate of production of O_2^- of 1.2 μmol dm^{-3} min^{-1}. The nbt reduction rate was measured for 300 s, both in the presence and absence of the copper(II) complexes. All experiments were carried out at 25 ± 0.2 °C using 1 cm thermostatted cuvettes, in which solutions were stirred magnetically. In separate experiments urate production by xanthine oxidase was monitored spectrophotometrically at 298 nm, ruling out any inhibition of xanthine oxidase activity by the systems investigated. The I_{50} values (the concentration which causes the 50% inhibition of nbt reduction; *i.e.* ΔA_{560} = 0.012 min^{-1}) of the copper(II) complexes at pH 6.8 and 7.8 are given in Table 4.

Results and Discussion

Thermodynamic Results.—The protonation constants for HL are reported in Table 5. In order to understand which sites are involved in each protonation step the values are compared with those of glycyl-L-histidyl-glycine (HL′) and glycyl-glycyl-L-histidine (HL″), *i.e.* tripeptides with histidine in non-terminal and terminal positions, respectively. For HL″ the protonation

Table 4 Superoxide dismutase activity of copper(II) complexes

Complex	I_{50}/μmol dm^{-3}
$[CuH_{-1}L] + [CuH_{-2}L]^{-}$ [a]	4.3
$[CuH_{-1}L] + [CuH_{-2}L]^{-}$ [b]	1.6
$[Cu(LysO)_2]^{2+}$ [c]	86
$[Cu(TyrO)_2]^{2+}$ [c]	45
Superoxide dismutase [c]	0.04

[a] pH 6.8. [b] pH 7.8. [c] Ref. 27; LysO = lysinate, TyrO = tyrosinate.

Table 5 Protonation constants for HL (at 25 °C and I = 0.1 mol dm^{-3} KNO_3) and some histidine tripeptides

Peptide	logK_{HL}	logK_{H_2L}	logK_{H_3L}	logK_{H_4L}	Ref.
HL [a]	8.00(2)	6.95(2)	6.00(3)	2.57(3)	This work
HL'	7.98	6.35	—	2.72	10
	7.995	6.50	—	3.08	13
HL'' [b]	7.96	6.64	—	2.92	10

[a] σ In parentheses. [b] HL'' = Gly-Gly-L-His.

Table 6 Stability constants for copper(II)–HL complexes at 25 °C and I = 0.1 mol dm^{-3} (KNO_3)

	log β*
$Cu^{2+} + L^{-} + H^{+} \rightleftharpoons [CuHL]^{2+}$	15.35(3)
$Cu^{2+} + L^{-} \rightleftharpoons [CuL]^{+}$	12.626(3)
$Cu^{2+} + L^{-} \rightleftharpoons [CuH_{-1}L] + H^{+}$	7.01(1)
$Cu^{2+} + L^{-} \rightleftharpoons [CuH_{-2}L]^{-} + 2H^{+}$	−0.05(3)

* σ in parentheses.

constant of the imidazole nitrogen is higher than that in HL', suggesting that the imidazole nitrogen of the terminal histidine residue is more basic than that of the histidine in a non-terminal position. Hence, we tentatively attribute the second protonation step to the nitrogen of the C-terminal imidazole and the third step to the protonation of the first imidazole nitrogen, even if these constants are very likely macro-constants containing contributions from the protonations of both histidines. The first and the fourth protonation steps refer to the amino nitrogen and the carboxylic oxygen, respectively.

For the copper(II)–HL system the following species were considered: $[CuHL]^{2+}$, $[CuL]^{+}$, $[CuH_{-1}L]$, $[CuH_{-2}L]^{-}$, $[CuH_2L]^{3+}$, $[Cu_2H_{-1}L]^{2+}$, $[Cu_2H_{-2}L]^{+}$, $[Cu_2L_2]^{2+}$, $[Cu_2H_{-1}L_2]^{+}$ and $[Cu_2H_{-2}L_2]$, with the first three species as the base model and the other species introduced, as usual, in different combinations. Previously studied hydrolytic equilibria [28] were also included in the data processing. The statistical parameters were improved by adding $[CuH_{-2}L]^{-}$ to the base model (SUPERQUAD: σ = 5.2 and 1.6 and χ^2 = 18.5 and 5.9 without and with this species, respectively). All the other species were always rejected as being negative or excessive by the program when added to the base model. The species $[CuHL]^{2+}$ never exceeded 5% of the total copper(II).

A species distribution diagram (Fig. 1) shows the major species in the pH range 3.0–5.5 is $[CuL]^{+}$, which has a high stability constant (Table 6) compared to other similar copper(II) di- or tri-peptide complexes. By comparing this value with those for copper(II)–L-histidyl-L-histidine or L-histidyl-D-histidine (His-His) complexes [14] the donor atoms involved in the co-ordination and the reason for the large log β value may be deduced. In $[CuL'''']^{+}$ (HL'''' = His-His) (log β = 11.10), it is proposed that copper(II) binds to N^{-}, NH_2 and N(3) (imidazole) by taking into account the spectroscopic data also.[14] Analogously, we can assume that the $[CuL]^{+}$ species is an NNN bound complex with the terminal NH_2, the

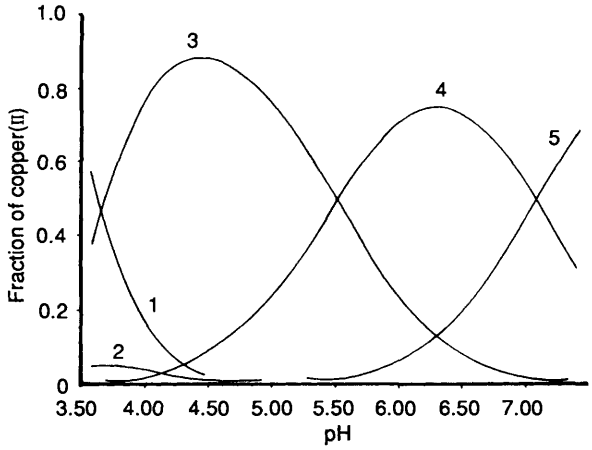

Fig. 1 Species distribution diagram obtained by pH-metric measurements on the Cu–HL system at 25 °C, I = 0.1 mol dm^{-3} (KNO_3); [HL] = 4.11 mmol dm^{-3}. 1, Free metal ion; 2, $[CuHL]^{2+}$; 3, $[CuL]^{+}$; 4, $[CuH_{-1}L]$; and 5, $[CuH_{-2}L]^{-}$

deprotonated peptide nitrogen, and the first imidazole nitrogen [*i.e.* not the C-terminal imidazole as in the copper(II)–His-His complex] binding to the metal. This difference can contribute to the larger value of log β for $[CuL]^{+}$ compared to $[CuL'''']^{+}$. According to Brookes and Pettit,[29] the empirical formula $[CuL]^{+}$ represents a complex of real stoichiometry $M(HL)H_{-1}$ in which the terminal imidazole is protonated.

The similarity in the value of log β for the $[CuHL]^{2+}$ species and $[CuHL'''']^{2+}$ (log β = 15.77) suggests that the same donor atoms may be involved in the bonding to the metal ion, namely the terminal NH_2 and the N(3) of the first imidazole.

The formation of $[CuH_{-1}L]$ and $[CuH_{-2}L]^{-}$ is favoured more than the analogous species of tripeptides containing one histidyl residue;[10,13] for example for $[CuH_{-1}L]$ and $[CuH_{-2}L]^{-}$ log β values are 5.66 and −3.70, respectively.[13] However, on the basis of simple thermodynamic considerations, one would expect the fourth nitrogen involved in $[CuH_{-1}L]$ to be the imidazole nitrogen and that involved in $[CuH_{-2}L]^{-}$ to be the peptide nitrogen. In fact, the deprotonation constant of $[CuH_{-1}L]$ to give $[CuH_{-2}L]^{-}$ (7.06) is greater than what would be expected if complexation involved the imidazole nitrogen (6.95) from the histidine, since metal complexation generally decreases ligand protonation constants.

Spectroscopic Results.—Ueda *et al.*[15] have recently published a complete spectroscopic study (UV/VIS, CD and ESR) on copper(II) complexes with L-histidyl-glycyl-L-histidyl-glycine and L-histidyl-L-histidyl-glycyl-glycine. However, since only the pH values of the solutions were reported without any information on the stoichiometry of the actual species under study then unfortunately no comparison with our data can be made.

The ESR spectra were obtained from solutions containing copper(II) ions with HL in a 1:1 ratio at pH 4.5 and in the pH range 6.1–7.8. From room temperature ESR spectra isotropic g and A values were determined and are reported in Table 3. Fig. 2 shows two ESR spectra at different pH values where one absorbing species predominates. Other complex species may be present (Fig. 1), but their concentration is negligible compared to that of the major one. Fig. 2(*a*) presents the isotropic spectrum of $[CuL]^{+}$ at pH 4.5, while Fig. 2(*b*) shows the spectrum at pH 6.4, in which the prevalent species is $[CuH_{-1}L]$. The magnetic parameters are not very different, the hyperfine coupling constant of $[CuH_{-1}L]$ being only slightly lower than that of $[CuL]^{+}$. Both ESR spectra show superhyperfine structure with seven distinct lines, which can be attributed to three nitrogen donor atoms being involved in the co-ordination equatorial plane of the appropriate copper(II) complex. The pattern of the seven lines is quite

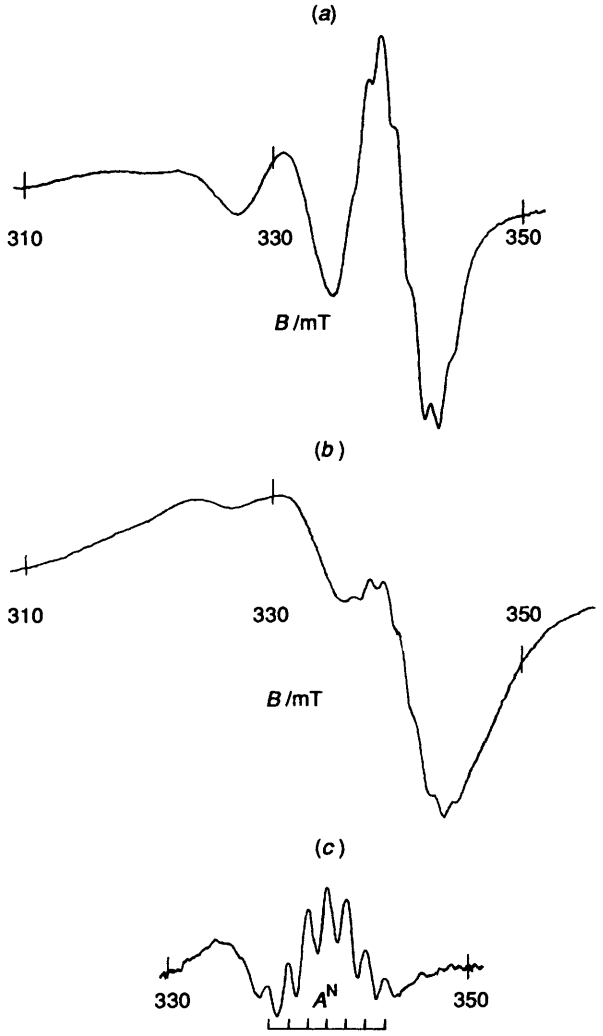

Fig. 2 Room temperature ESR spectra of the Cu–HL system in water (ligand to metal ratio 1.07:1, $[Cu^{2+}]$ = 3.84 mmol dm^{-3}) at (*a*) pH 4.5, $[CuL^+]$ = 3.35 mmol dm^{-3}, $[CuH_{-1}L]$ = 0.4 mmol dm^{-3}, $[CuH_{-2}L^-]$ = 2.6 μmol dm^{-3}; and (*b*) pH 6.4, $[CuL^+]$ = 0.13 mmol dm^{-3}, $[CuH_{-1}L]$ = 2.4 mmol dm^{-3}, $[CuH_{-2}L^-]$ = 0.77 mmol dm^{-3} (microwave frequency = 9.761 GHz; microwave power = 50 mW; modulation frequency = 100 kHz; field modulation amplitude = 2.5 G; time constant = 200 ms, scan time = 500 s); and (*c*) second derivative spectrum at pH 4.5 (modulation frequency = 12.5 kHz, time constant = 500 ms, scan time = 200 s)

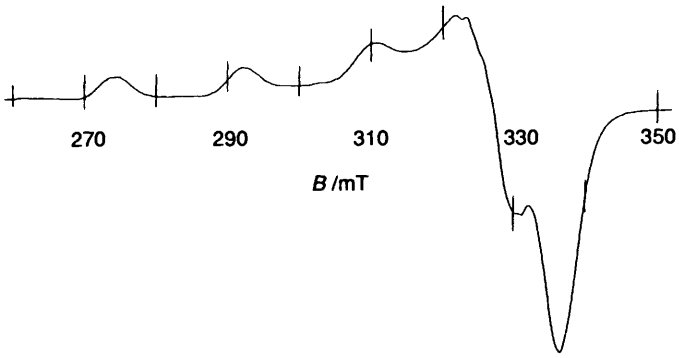

Fig. 3 Frozen solution ESR spectrum of the Cu–HL system (ligand to metal ratio 1.07:1) in water–methanol (85:15) (aqueous solution pH 4.5) at 150 K (microwave frequency = 9.443 GHz, microwave power = 20 mW, modulation frequency = 100 kHz, field modulation amplitude = 2.5 G, time constant = 500 ms, scan time = 500 s)

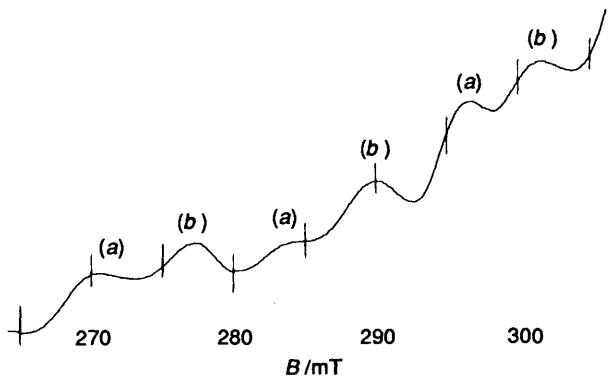

Fig. 4 Frozen solution ESR spectrum of the Cu–HL system (ligand to metal ratio 1.07:1) in water–methanol (85:15) (aqueous solution pH 7.8) at 150 K (only the parallel absorption lines are shown) (*a*) $[CuH_{-2}L]^-$, and (*b*) $[CuH_{-1}L]$ (microwave frequency = 9.443 GHz, microwave power = 20 mW, moculation frequency = 100 kHz, field modulation amplitude = 8 G, time constant = 500 ms, scan time = 500 s)

regular indicating that the three nitrogen donors are quasi-equivalent.

The frozen solution spectrum at pH 4.5 is characterized by a single species (Fig. 3), the parameters of which were attributed to the $[CuL]^+$ complex. The low $g_{\|}$ value and the high $A_{\|}$ constant are characteristic of copper(II) complexes with three or four nitrogen atoms in the equatorial plane. However, the room temperature ESR spectrum showing a superhyperfine structure with a seven-line pattern indicates that three nitrogen donors are involved in the co-ordination sphere of the copper(II) complex (Fig. 2), as already seen from the thermodynamic results. The co-ordination in the equatorial plane is probably completed by a water molecule. The high value of the parallel hyperfine constant suggests that this species has more distant apical solvent molecules.

In the pH range 6.1–7.8, the frozen solution ESR spectrum appears to be complicated by the presence of two other absorbing species (Fig. 4), the ratio of which depends on the solution pH. The change in the intensity ratio of the ESR signals due to the two species on going from pH 6.1 to 7.8 allows each spectrum to be attributed to one of the two species present in the system. From the speciation study, the formation of $[CuH_{-2}L]^-$ increases on increasing the pH of the solution. Hence, the absorptions were assigned to $[CuH_{-1}L]$ and $[CuH_{-2}L]^-$, the magnetic parameters of which are reported in Table 3. It is important bear in mind that above pH 6.1 the concentration of $[CuL]^+$ is negligible. The $[CuH_{-1}L]$ complex shows an increase in $g_{\|}$ and $g_{\perp}$ values and a dramatic decrease in the $A_{\|}$ value compared to $[CuL]^+$. Since at pH 6.4 $[CuH_{-1}L]$ is the prevalent species and the room temperature ESR spectrum shows seven superhyperfine lines, it may be thought that the second deprotonated imidazole nitrogen atom is forced to co-ordinate to copper(II) in one of the two apical positions, thus leading to a square-pyramidal geometry. The shifts in the values of the magnetic parameters[30] would be merely due to the formation of a five-co-ordinated adduct in which the set of donor atoms involved on the equatorial plane was not substantially changed. The low value of $A_{\|}$ and the relatively high $g_{\perp}$ value are suggestive of apical interaction.[31] Hence, in $[CuH_{-1}L]$ the amino nitrogen, the first peptide nitrogen, the first imidazole nitrogen and the water molecule form the equatorial plane, and the second imidazole nitrogen links apically to copper(II).

In the species $[CuH_{-2}L]^-$ the second peptide nitrogen is deprotonated. The much higher $g_{\|}$ value and the relatively low $A_{\|}$ hyperfine constant [with four nitrogen atoms to be accommodated around the copper(II) ion and the complex being negatively charged] and the rather low $g_{\perp}$ value indicate quite a distorted geometry. This could be due either to the

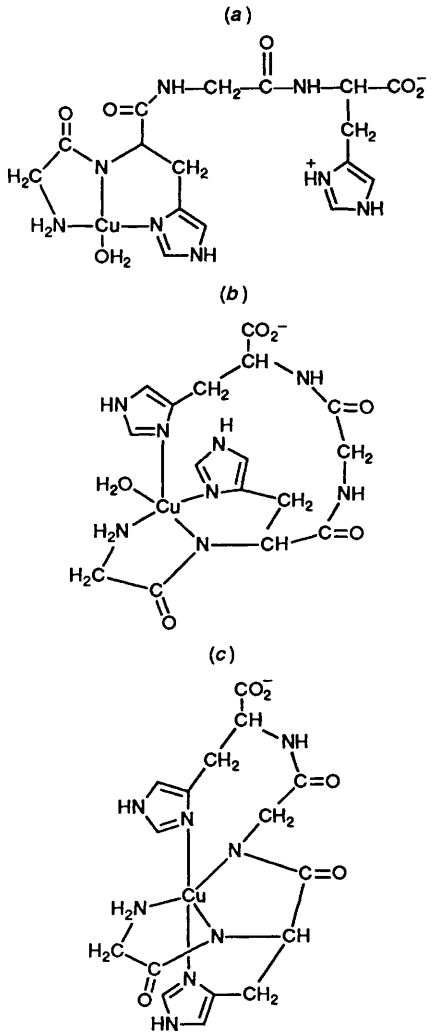

Fig. 5 Proposed structures of $[CuL]^+$ (*a*), $[CuH_{-1}L]$ (*b*), $[CuH_{-2}L]^-$ (*c*)

formation of a tetrahedrally distorted plane[32] with four nitrogen atoms (two from peptide groups, one from the amino group and the fourth from an imidazole group) in a distorted square-pyramidal geometry, or a distorted trigonal bipyramid with two imidazole nitrogen donor atoms along the apical sites and two peptide nitrogens with the amino nitrogen in the equatorial positions, *i.e.* the geometry of $[CuH_{-2}L]^-$ is intermediate between a tetrahedrally distorted square pyramid and a trigonal bipyramid. The latter geometry could result in the low $g_\perp$ value, which approaches that of the free electron, as would be expected for a copper(II) complex with a d_{z^2} orbital mixing into the ground state.[33]

The differences in the frozen solution ESR spectra of the three species were not as evident from the results of the room temperature study. It may be that the low temperature experiments show differences which are somewhat levelled by vibrational and rotational motion at room temperature. This behaviour, which is a little uncommon for copper(II) complexes, is probably due to the great flexibility of the ligand as already suggested by the NMR study.

Visible optical spectra were obtained for solutions containing the copper(II) ion and HL in equimolar ratio, varying the pH of the solution. The complex $[CuL]^+$ shows an absorption maximum in the visible region at 606 nm (ε = 58 dm^3 mol^{-1} cm^{-1}) which is typical of a CuN_3 chromophore as already found for $[CuL'''']^+$ (615 and 620 nm for the pure and the *meso* isomers, respectively).[14] On raising the pH of the solution to 6.5 a blue shift from 606 nm is observed, due to the formation of $[CuH_{-1}L]$ and $[CuH_{-2}L]^-$. From the speciation study the concentration of each of the latter two species may be obtained and hence their absorption maxima calculated at 574 (ε = 54) and 575 nm (ε = 72 dm^3 mol^{-1} cm^{-1}), respectively. The blue shifts are the consequence of the successive co-ordination of the imidazole and peptide nitrogens, in that order, to the copper(II) ion. The difference in the ε values and the similar λ_{max} value (despite further nitrogen co-ordinated in $[CuH_{-2}L]^-$) reinforce the conclusion drawn from the ESR study. In fact, a lower ligand field is expected for highly distorted arrangements as well as an increase in the intensity of the absorption bands.[34,35]

The CD spectra were obtained under the same experimental conditions as the absorption spectra, but only at pH 4.5 where the major species is $[CuL]^+$. The CD spectrum of this species shows three bands (Table 2). The two in the visible region at 608 and 502 nm are assigned to $d_{xy} \longrightarrow d_{x^2-y^2}$ and $d_{xz,yz} \longrightarrow d_{x^2-y^2}$ transitions, respectively. The band at 330 nm is assigned to charge transfer from an imidazole nitrogen to copper(II). These data are virtually coincident with those previously reported[13,15] for the complex $[CuH_{-1}L']$ (Table 2), in which it has been proposed that copper(II) is co-ordinated by three nitrogens, namely an imidazole, an amine and a peptide nitrogen. This confirms the structures proposed on the basis of thermodynamic and ESR data which are shown in Fig. 5.

Superoxide Dismutase-like Activity.—Many low molecular weight complexes of copper(II) are known to be catalysts for superoxide dismutation.[18,27] The overall reaction is shown in equation (1). As already underlined in previous studies,[18,36] the

$$Cu^{II} + 2O_2^- + 2H^+ \longrightarrow Cu^{II} + H_2O_2 + O_2 \quad (1)$$

knowledge of the correct speciation of the system under working conditions (*i.e.*, the knowledge of all the species actually present in the solution under study) plays a central role in the determination of any reasonable structure-activity relationship.

We measured the catalytic activity of the complexes with oxygen radicals at pH 6.8 and 7.8, under conditions described in the Experimental section. As shown in Fig. 1, $[CuH_{-1}L]$ is the major species at pH 6.8 (63.4%), but at pH 7.8 the solution contains only 15% of this species and 85% of $[CuH_{-2}L]^-$. Using DISDI,[25] the concentration of free copper(II) ion was calculated to be always less than 0.05% under the conditions described here, and that of copper(II) complexes of either phosphate or xanthine even lower. The catalytic activity measured in the presence of an excess of ligand was identical to that with no excess, thus excluding any contribution from the ligand. Our results show higher activity at pH 7.8 than at pH 6.8 (Table 4). It is worth noting that the increase in superoxide dismutase-like activity parallels the increase in the concentration of the $[CuH_{-2}L]^-$ complex and at pH 7.8 both the percentage of this species and the activity with superoxide are about 2.5 times higher than those at pH 6.8. This suggests either a lack of activity of the $[CuH_{-1}L]$ species or a higher activity of $[CuH_{-2}L]^-$.

The different behaviour of the two species toward the O_2^- radical ion may be due to differences in their structures.[18,36,37] Two important requirements for the superoxide dismutase-mimicking of copper(II) complexes are: (*i*) the presence of at least one free co-ordination site to allow the reaction with the superoxide anion, and (*ii*) the possibility for stabilization of the copper(I) in a pseudo-tetrahedral arrangement. Therefore, given the geometrical features of the species present at the physiological pH values, inferred on the basis of thermodynamic and spectroscopic studies, the higher activity of $[CuH_{-2}L]^-$ can be rationalized by the highly distorted geometry of this species, which is probably able to stabilize copper(I). However, the presence of $[CuH_{-1}L]$ has little or no influence on the superoxide dismutase-like activity which is probably due to the co-ordination environment of this species (a square pyramidal

geometry of four nitrogen and an oxygen from a water molecule) that may prevent the attack by the O_2^- radical ion. This is probably because the copper(II) is tilted away from the equatorial plane and buried in the cavity caused by the tetrapeptide as a consequence of the axial co-ordination of the terminal histidine to the metal ion. It is possible that in $[CuH_{-2}L]^-$ the attack of the O_2^- occurs in an equatorial position, *via* an expansion of the co-ordination sphere from five to six.

Acknowledgements

We thank the Consiglio Nazionale delle Ricerche (CNR) Progetto Finalizzato Chimica Fine II and the Ministero della Universitá e della Ricerca Scientifica e Tecnologica (MURST) for partial support.

References

1 B. Sarkar and T. P. A. Kruck, in *Biochemistry of Copper*, eds. J. Peisach, P. Aisen and W. E. Blumberg, Academic Press, New York, 1966, p. 183.
2 A. A. Gewirth, S. L. Cohen, H. J. Schugar and E. I. Solomon, *Inorg. Chem.*, 1987, **27**, 1133.
3 J. McCracken, S. Pernber, S. J. Benkovic, J. J. Villafranca, R. J. Miller and J. Peisach, *J. Am. Chem. Soc.*, 1988, **110**, 1069.
4 N. Ito, S. E. V. Phillips, C. Stevens, Z. B. Ogel, M. J. McPherson, J. N. Keen, K. D. S. Yadav and P. F. Knowles, *Nature (London)*, 1991, **350**, 87.
5 C. L. Davey, *Arch. Biochem. Biophys.*, 1960, **89**, 296.
6 C. L. Davey, *Arch. Biochem. Biophys.*, 1960, **89**, 303.
7 L. Pickart and M. M. Thaler, *J. Cell Physiol.*, 1980, **102**, 129.
8 T. Sakurai and A. Nakahara, *Inorg. Chem.*, 1980, **19**, 847.
9 J. Laussac, R. Haran and B. Sarkar, *Biochem. J.*, 1983, **209**, 533.
10 E. Farkas, I. Sovago, T. Kiss and A. Gergely, *J. Chem. Soc., Dalton Trans.*, 1984, 611.
11 G. Arena, V. Cucinotta, S. Musumeci, R. Purrello and E. Rizzarelli, *Ann. Chim. (Rome)*, 1984, **74**, 399.
12 A. Ensuque, A. Demaret, L. Abello and G. Lapluye, *J. Chem. Phys.*, 1987, **84**, 1013.
13 P. G. Daniele, O. Zerbinati, V. Zelano and G. Ostacoli, *J. Chem. Soc., Dalton Trans.*, 1991, 2711.
14 C. E. Livera, L. D. Pettit, M. Bataille, B. Perly, H. Kozlowski and B. Radomska, *J. Chem. Soc., Dalton Trans.*, 1987, 661.
15 J. Ueda, N. Ikota, A. Hanaki and K. Koga, *Inorg. Chim. Acta*, 1987, **135**, 43.
16 Y. Koijma, *Chem. Lett.*, 1981, 61.
17 G. Arena, R. P. Bonomo, G. Impellizzeri, R. M. Izatt, J. D. Lamb and E. Rizzarelli, *Inorg. Chem.*, 1987, **26**, 795.
18 C. Amar, E. Vilkas and J. Foos, *J. Inorg. Biochem.*, 1982, **17**, 313.
19 S. Goldstein, G. Czapski and D. Meyerstein, *J. Am. Chem. Soc.*, 1990, **112**, 6489.
20 H. Zhuang and C. Lu, *Huaxue Xuebao*, 1990, **22**, 593; *Chem. Abstr.*, 1991, **115**, 178055c.
21 C. Beauchamp and I. Fridovich, *Anal. Biochem.*, 1971, **44**, 276.
22 A. Flaschka, *EDTA Titrations*, Pergamon, London, 1959.
23 G. Arena, C. Rigano, E. Rizzarelli and S. Sammartano, *Talanta*, 1979, **26**, 1.
24 P. Gans, A. Vacca and A. Sabatini, *J. Chem. Soc., Dalton Trans.*, 1985, 1195.
25 R. Maggiore, S. Musumeci and S. Sammartano, *Talanta*, 1976, **23**, 43.
26 J. R. Pilbrow and M. E. Winfield, *Mol. Phys.*, 1973, **26**, 1073.
27 U. Deuschle and U. Weser, *Prog. Clin. Biochem. Med.*, 1985, **2**, 97 and refs. therein.
28 G. Arena, R. Cali, E. Rizzarelli and S. Sammartano, *Thermochim. Acta*, 1976, **16**, 315.
29 G. Brookes and L. D. Pettit, *J. Chem. Soc., Dalton Trans.*, 1975, 2112.
30 R. P. Bonomo, F. Riggi and A. J. Di Bilio, *Inorg. Chem.*, 1988, **27**, 2510.
31 D. Kivelson and R. J. Neiman, *J. Chem. Phys.*, 1961, **35**, 149.
32 U. Sakaguchi and A. W. Addison, *J. Chem. Soc., Dalton Trans.*, 1979, 600.
33 B. J. Hathaway and D. E. Billing, *Coord. Chem. Rev.*, 1970, **5**, 143.
34 A. B. P. Lever, *Inorganic Electronic Spectroscopy*, Elsevier, New York, 1984.
35 B. N. Figgis, *Introduction to Ligand Fields*, Interscience, Wiley, New York, 1966.
36 L. L. Costanzo, G. De Guidi, S. Giuffrida, E. Rizzarelli and G. Vecchio, *J. Inorg. Biochem.*, in the press.
37 M. Linss and U. Weser, *Inorg. Chim. Acta*, 1987, **138**, 163.

Received 25*th September* 1992; *Paper* 2/05178H